

H. KADDOURI*, M. MAKOWSKA-JANUSIK,
J. BERDOWSKI and I.V. KITYK

**Institute of Physics, Laboratoire LP2A, University of Perpignan, Perpignan, France
Institute of Physics WSP Częstochowa, Al. Armii Krajowej 13/15, Częstochowa, Poland*

UV-Induced SHG in $\text{SiO}_x\text{C}_{1-x}\text{N}$ Nanocrystals

1. Introduction

One can recently observe increasing interest in semiconductor nanocrystals due to their important size-dependent electronic and optical properties [1–3]. Among the semiconductors, necessary technology is developed for oxynitrides of the SiO_xN_y type [4]. Varying content of oxygen, nitrogen or N/O ratio, one can operate by value of an effective energy gap, conduction band barrier, dielectric constants, etc. [5]. Quite recently [6,7], it was revealed that interfaces between the silicon oxides (nitrides) and surrounding substrates could prefer appearance of second-order nonlinear optical effects, particularly of optical second harmonic generation (SHG). Theoretical simulations [8, 9] predict possibility to enhance nonlinear optical susceptibilities in the semiconductor nanocrystallites. Particularly the prevailing quantum chemical simulations show that by replacing oxygen by carbon one can expect enhanced output SHG.

For a wide application of the nanocrystallites in optoelectronics, there appears requirement to prepare specimens of high-quality (homogeneity). The specimens are usually prepared as films deposited on a dielectric substrates. In this case, a high light scattering background appears to be main problem. To eliminate this difficulty, one can suggest a guest-host polymer technique [10–12] to be applied in the case of the powder-like nanocrystallites. Such setup has been used for $\text{Sn}_2\text{P}_2\text{S}_6$ semiconductor nanocrystallites embedded in the oligoetheracrylate photopolymer matrices [13]. Better parameters (low light scattering losses, optical homogeneity, higher transparency, etc.) are achieved when external electric field favors orientation of the embedded pow-

der-like nanocrystallites. Another important strategy for enhancement of the nonlinear optical susceptibilities consists in additional photoexcitation of the chromophores (in our case, the nanocrystallites) to enhance appropriate dipole moment matrix elements that determines the output nonlinear optical susceptibility [14].

Among the semiconducting nanocrystallites, the SiOCN ones have been chosen because preparation techniques of these specimens with desired C/O were sufficiently developed [4, 5]. Calculated electron charge density distributions in the oligoetheracrylate photopolymers [15–17] indicate a good match of the polymers to the SiOCN semiconductors because their dipole moments are collinear. Another important advantage of the oligoetheracrylate matrices consists in their good mechanical and features [18], determining photoinduced response of the investigated materials.

To eliminate necessity to depose the SiOCN films on Si substrates, we have proposed to use the nanocrystallite-like specimens incorporated into the photopolymer matrices. The oligoetheracrylate photopolymers have been chosen for the following reasons:

- good optical transparency,
- low scattering background,
- parallel directions of dipole moments for ground and excited states for photopolymers and embedded SiOCN nanocrystallites,
- low proper nonlinear optical susceptibilities.

2. Experiment

In present paper, we present experimental results for the photoinduced nonlinear optical phenomena in the SiOCN nanocrystallites embedded in the oligoetheracrylate photopolymer matrices. The SiOCN powder-like nanocrystallites have been prepared using source gases of high purity (SiH_2Cl_2 , NH_3 , CO_2 and N_2O) and varying $\text{N}_2\text{O}/\text{CO}_2$ source gases ratio. A growth rate was dependent on the C/O/N ratio. The specimens were thermo-annealed within a temperature range between 578 K and 1346 K. Continuously varying the ratio of input components, the SiOCN nanocrystallites of different C/N ratio have been obtained. The nanocrystallite sizes were changed by varying deposition time. Homogeneity and stoichiometry of the composites were measured using an Auger and EXAFS electron spectroscopy. The prepared nanocrystallite sizes have been varied within the 10 – 50 nm.

2.2. Photoinducing nonlinear optical measurements

The principal set-up for measurements of the PISHG was the same as described in the Ref. 1. As a source of the photoinduced changes UV nitrogen laser beam ($\lambda = 337 \text{ nm}$) with a photon flux varying within $10^{17} - 10^{20}$ photons/cm² has been used. Upper power restriction was caused by a necessity to avoid sample heating. An intensity at specimen position was measured using a commercial fast-response joulemeter (Genetic, Inc., model ED-200).

As a source of the probe beam we used unfocused beam from a single-mode picosecond YAG-Nd laser ($\lambda = 1.06 \mu\text{m}$), with a power about 30 MW and pulse time duration varying within the 10 – 38 ps. The set-up allows to rotate the incident angle θ of the photoinducing beam relative to the specimen surfaces. Polarisation of the photoinducing as well of the probing light beams have been changed by polarisers P1 and P2. The signals of these two lasers were synchronised by a time-electronic synchroniser S.

Separation between the output SHG, probe and pump (photoinducing) light was achieved using grating monochromator (SP) (spectral resolution up to 7 nm/mm) and filter (F). Laser beam spot diameter was varied within the 60 – 1580 μm . Such wide range of the beam diameter variation has been caused by a necessity to achieve the optimal phase matching synchronism conditions for the investigated glasses. The latter were achieved (fulfilled) due to rotation of the incident photoinducing UV-laser beam direction towards the surface of the specimen. As a consequence the effective interaction lengths were changed. The control of the two laser beam intensities was done using the photomultiplier (PM) gathering the signals split by the two beamsplitters (BS). Effective interaction lengths have been varied within the 5 – 7 mm depending on the angle of incident photoinducing beam θ . The maximal output PISHG signal was achieved for the incident UV-laser beam angles lying within the 8 – 12° and for parallel polarisation of the photoinducing and probing beams. These parameters are essentially dependent on the photoinduced birefringence changes (up to 0.26). However, due to gaussian-like shape of the UV-incident light we have a non-homogeneity in the coherence length values and the corresponding phase synchronism conditions are fulfilled within the large range of the incident angles changes.

- PISHG intensity was detected using a PMD –33M photomultiplier working in the digital quantum regime. The output signal was observed only for the effective χ_{zzz} tensor. Z-direction corresponds to polarisation of the photoinducing UV nitrogen beam. All the measurements have been started for the pure silica glasses. Afterwards the PISHG experiments were done using the same conditions for the

Yb,Er-doped glasses. As a consequence, a comparison with the PISHG effects only due to the *RE* presence within the similar conditions was possible. To ensure the same conditions of the measurements surface states, scattering losses and averaged non-homogeneity have been monitored. Moreover, to eliminate non-homogeneity connected with the non-uniform distribution of the *RE* ions averaging procedure consisting in the scanning measurements in more than 85 points of the investigated glasses was done. All the obtained data were treated using the $\chi^{(2)}$ Student statistics not worse than 0.02 [8]. The measurements were done in the single-pulse regime, with a pulse frequency repetition of 12 Hz. As an intensity standard a quartz single-crystal cell in the plane of the optic axis has been used. Simultaneously for every measured point the incident angle θ was varied in order to fulfil the phase matching conditions corresponding to the maximal output PISHG. The self-focused beam diameter (about 1.24 μm) was of a gaussian-like form with the half-width about 72%. Single-mode regime of laser generation was applied to eliminate inter-mode competition and different kinds of soliton-like effects. Simultaneously the reflected optical beams (both incident as well frequency-doubled) have been measured to extract an influence of near-the surface effects. Time-dependent PISHG signals were measured by means of the high-time-resolved spectroanalyser SA-107. Time synchronisation between the photoinducing and probing beams was achieved within the time ranges about 200 fs.

- For performance of the temperature-pressure dependent PISHG measurements all the specimens have been kept in the thermo-chamber, that allows to vary the temperature within the 4.2 – 300 K with stabilisation about 0.02 K. The pressures up to the 20 GPa have been changed using the hydrostatic gaseous media set-up similarly as described in the Ref. 8 with a step about 0.2 GPa.

Electrooptically operated delaying line made of a $\text{Li}_2\text{B}_4\text{O}_7$ single crystal has been applied for operation by the pump-probe time delay. This allows us to vary the delaying time with a time resolution not worse than 0.6 ps. As a consequence, any misbalance between the laser beams can be corrected. For each specimen, the measurements have been performed in more than 95 points of specimen surface to achieve a reliable statistical averaging within a χ^2 Student distribution (not worse than 0.02).

Photodetection has been carried out by a digital high-resolution multiplier RCA-121 and FE-124-H connected with a boxcar gate of about 480 ps. A grating monochromator SPM-3 (with spectral resolution of 7 nm/mm) has been used to separate green doubled frequency signal ($\lambda = 0.53 \mu\text{m}$) from the

source YAG:Nd laser ($\lambda = 1.06 \mu\text{m}$) background. The pump and probe signals were detected independently by connected synchronised photomultipliers (PM).

The oligoetheracrylate photopolymer alloys have been prepared using the mixing of the particular components in the such contents in order to achieve the minimal scattering. These photopolymers are convenient for the continuous variation of the refractive indices [13].

3. Results and Discussions

The performed investigations have shown that the output second harmonic generation during the photoinducing process cause an increase of the output SHG signal from $2 \cdot 10^{-5}$ up to the $3 \cdot 10^{-4}$ comparing with the incident angle.

The photoinducing effect causes the following processes:

1. Optical poling (polarization of the dipoles in the ground and UV-induced states);
2. Photocarrier redistribution leading to the effective shift of the Fermi energy level;
3. Appearance of the photoinduced matrix dipole moments contributing additionally to the output SHG;
4. Increasing of the coherence lengths to due to the photoinduced birefringence.

The optical photoorientation of the excited states is essentially more convenient (needs less electric strength) than the ground states dipoles. This is caused by a higher delocalisation of the UV-excited states comparing with the ground state ones. In the case of the considered materials the estimations done on the ground of the difference dipole moments in the excited and ground states predict enhancement of the output nonlinear susceptibility at least 12% for the SiOCN and 18% for the oligoetheracrylate materials. The output second harmonic generation signal averaged over the mentioned materials is equal about $2 \cdot 10^{-5}$. The measurements have shown that inhomogeneity of the specimens in respect to the refractive and extinction coefficients was less than $10^{-1}\%$. In order to avoid the unexpected inhomogeneous distribution of the output SHG signal we have measured the output SHG in more than 75 points of the investigated polymer surfaces. During the evaluations of the second-order nonlinear optical susceptibility we have used an expression:

$$I_i^{(2\omega)} = 2\mu_0^{3/2} \epsilon_0^{1/2} S \omega^2 I_j^{(\omega)} I_k^{(\omega)} |\chi_{ijk}(\omega, \omega; 2\omega)|^2 d^2 [\sin(\Delta k d/2)/(\Delta k d/2)]^2, \quad (1)$$

where $S = (\pi R_0^2 n_k(\omega) n_j(\omega) n_i(2\omega))^{-1}$; $n_{i,j,k}(\omega)$ – i,j,k -th components of the refractive index for the corresponding crystallographic components; R_0 – radius of the SHG source beam; $\chi_{ijk}(\omega, \omega; 2\omega)$ – second order nonlinear optical susceptibility determining the interactions of the two beams with frequencies about ω that generate doubled frequency 2ω ; μ_0 and ϵ_0 magnetic and dielectric susceptibilities, respectively; $\Delta k = k(2\omega) - 2k(\omega)$ – wave-vector synchronism difference between the output and source wave; d – thickness of the specimen; $I_{j,i,k}^{(\omega, 2\omega)}$ – j,i,k -th light polarisation components of the appropriate frequencies.

The UV-induced optical Kerr effect causes additional birefringence determined by the linear and quadratic electrooptic effects:

$$\Delta n_{i,j} = r_{ijk} E_j^{(0,\omega)} E_k^{(0,\omega)} \quad (2)$$

where $E_{k,j}^{(0,\omega)}$ – effective electrostatic k,j -th components of the UV-photoinduced wave; r_{ijk} – linear electrooptics (Pockels static electric field component).

Our evaluations show that the PI birefringence is maximal for the photo-inducing beam about 1.2 GW/cm^2 , contrary to the 1.7 GW/cm^2 for the photopolymer and the 1.5 GW/cm^2 nanocrystallite powders deposited on the Si<111> substrates. Using of the silicon substrates is limited by the narrow band gaps of the silicon. This fact indicates the dominant role played by the interfaces in the observed photoinducing effects. It is well known that key role in the nonlinear optical susceptibilities play ground state dipole moments $\mu_{\alpha,\beta}$. However, in the case of the UV excitation an essential contribution of the excited dipole moments begins to give significant role.

Our quantum chemical calculations performed for the oligoetheracrylate photopolymers [15–17] have shown that the excited dipole moments are directed parallel with respect to the ground states dipole moments. As a consequence we have assumed that the interface between the nanocrystallites and the polymer should lead to an enhancement of the output nonlinear optical susceptibility both for the optical Kerr as well for the optical second harmonic generation. In the Table 1 are presented dipole moments of the particular structural fragments of the presented composites before and after the UV photoillumination.

Table 1. Dipole moments (in Debyes) due to the electronic and vibration states

N	OEA LHeT	SiCON(averag) LHeT	Interface LHeT	OEA RT	SiCON(averag) RT	Interface RT
before	1.6	2.35	4.67	1.35	2.12	4.25
after	1.86	2.67	5.76	1.67	2.24	5.03

Measured dependencies of the photoinduced SHG intensity as a function of the photoinducing nitrogen laser pump flux I and C/N are shown in Fig. 1. With increasing power of the photoinducing nitrogen laser pulses, the SHG maximum output signal increases and achieves its maximum at pump photon flux of about 1.93 GW/cm^2 . It is necessary to underline that the maximum photoinduced SHG is achieved for the C/N ratio of about 0.92 and is equal to about $3.82 \pm 0.11 \text{ pm/V}$. The measurements have been carried out for different concentrations of the nanocrystallite chromophores.

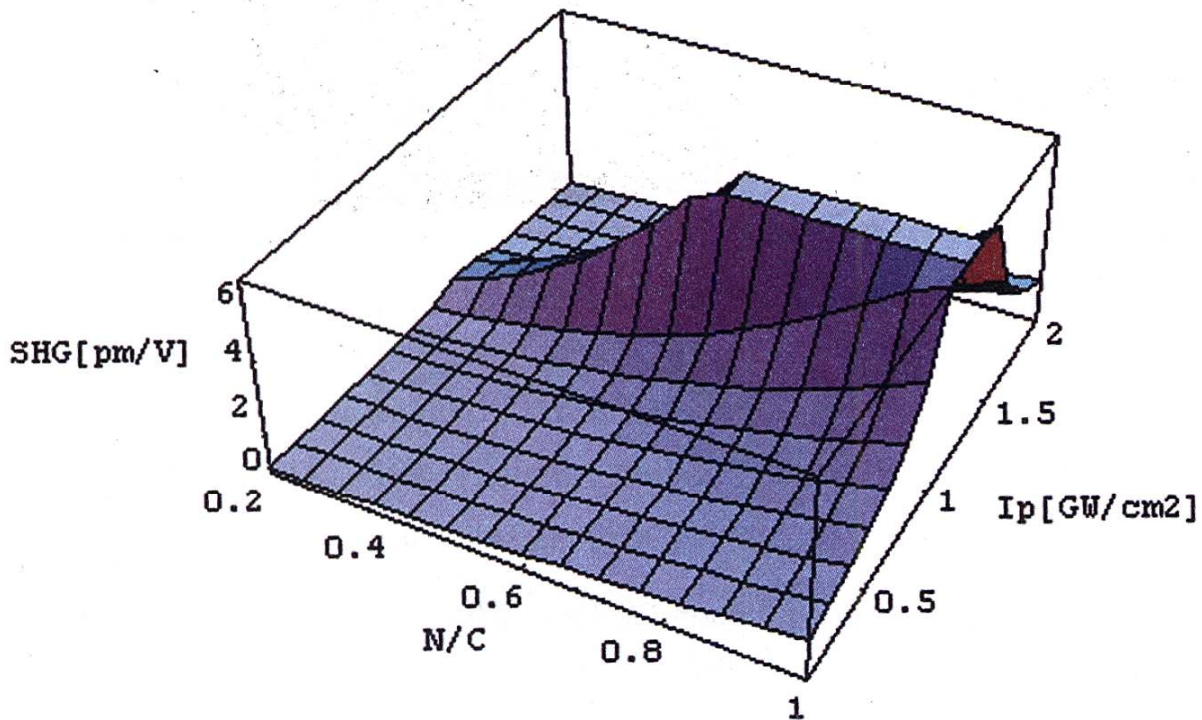


Fig. 1. Dependence of photoinduced SHG in SiCON nanocrystallites versus N/C ratio and photoinducing UV-laser flux I

The investigations have shown that the optimal concentration of the embedded SiCON nanopowders lies between 1.8% and 2.7%. We have found that for the concentrations about 2.7% the corresponding PISHG signal is saturated. The latter is caused by formation of the agglomerates due to electrostatic interactions. The maximal output SHG signals have been achieved for a delaying time between the photoinducing and probing beam of about 16 ps. The main output SHG is observed for χ_{222} tensor components (where axis # 2 is parallel to the UV-photoinducing laser polarisation and applied electropoling field). All presented data are obtained for temperatures above 4.2 K and

lower than 50 K because the long-range non-centrosymmetry is destroyed for higher temperatures. The Maker fringe oscillations are better for the angles 4–35°. All the data were averaged over the specimen volumes.

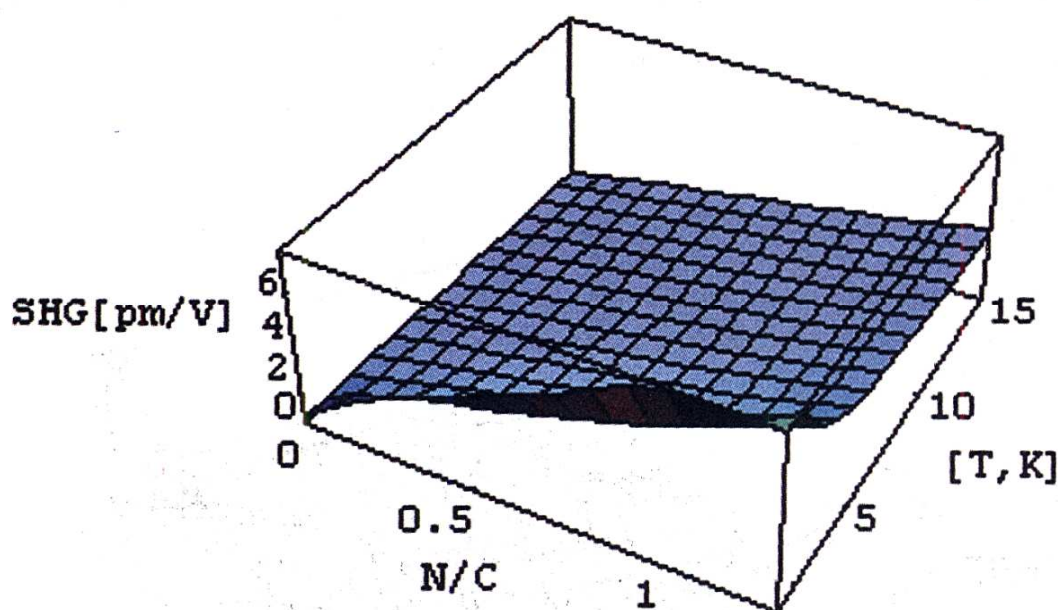


Fig. 2. Dependence of photoinduced SHG in SiCON nanocrystallites versus N/C ratio and temperature T

Temperature measurements of the photoinducing SHG (for the photoinducing powers lying within the 1.2–2.3 GW/cm²) are shown in Fig. 2. One can conclude that decreasing temperature favours the increase of SHG at low temperatures, similarly as in amorphous chalcogenide glasses [19]. Increase of the N content shifts the photoinduced SHG towards lower temperatures (contrary to the photoinducing dependencies). The observed behaviour reflects a probable competition between the long-range temperature reorientation and space interaction between particular SiON nanocrystallites due to the intracrystallite non-centrosymmetry.

In order to evaluate possible role of the photopolymer oligoetheracrylate matrices, analogous measurements on the SiON films deposited on Si<111> substrates have shown that the maximal output SHG signal were four times smaller [20]. The oligoetheracrylate photopolymers have vanishing values of the SHG [15–18]. Therefore, the main contribution to the nonlinear optical

susceptibility comes from the guest-host interfaces. Theoretical simulations of such contributions coming from particular fragments of the composites will be presented in a separate paper.

Our investigations have opened a possibility to use the SiON nanocrystals embedded within the photopolymer matrix as new materials for nonlinear optics. However, the nonlinear effects are below 0.2 pm/V for the pure SiON nanocrystallites as well as for the oligoetheracrylate photopolymer. Therefore, the dominant role belongs to the surfaces separating the nanocrystallites and the photopolymer background.

References

- [1] C.R. Kagan, C.B. Murray, M. Nirmal and M.G. Bawendi, *Phys. Rev. Lett.* **76** (1996) 1517.
- [2] A. Mews, A.V. Kadavanich, U. Banin and A.P. Alivisatos, *Phys. Rev. B* **53** (1996) 13242.
- [3] D.J. Norris and M.G. Bawendi, *Phys. Rev. B* **53** (1996) 16338.
- [4] X. Guo and T.P. Ma, *IEEE Electron Device Letters* **19** (1998) 207.
- [5] T.P. Ma, *IEEE Transcation on Electron Devices* **45** (1998) 680.
- [6] H. Tanaka, G. Mizutani and S. Ushioda, *Surface Sci.* **402-404** (1998) 533.
- [7] J. Boness, G. Marowsky, J. Braum, G. Witte and H.G. Rubahn, *Surface Sci.* **402-404** (1998) 513.
- [8] R.W. Schoenlein, D.M. Mittleman, J.J. Shiang, A.P. Alivisatos and C.V. Shank, *Phys. Rev. Lett.* **70** (1993) 1014.
- [9] Y. Li, M. Takata and A. Nakamura, *Phys. Rev.* **57 B** (1998) 9193.
- [10] „Nonlinear Optical Effects in Organic Polymers”, NATO ASI Series, Series E: Applied Sciences, **162**, J. Messier, F. Kajzar, P. Prasad and D. Ulrich, eds. (Kluwer Academic Publishers, Dordrecht, 1989).
- [11] „Materials for Nonlinear Optics”, American Chemical Society, ACS Symposium Series, **455**, S.R.Marder, J.E.Sohn, and G.D.Stucky eds. (ACS, Washington, DC, 1991).
- [12] M. Kuzyk and C. Poga, in: „Molecular Nonlinear Optics”, 1994, **Ch. 7**, Academic Press, NY., 209.

- [13] I.V. Kityk, R.I. Mervinskii, J. Kasperczyk and S. Jossi, *Materials Letters*, **27** (1996) 233.
- [14] B. Sahraoui, I.V. Kityk, X. Nguyen Phu, P. Hudhomme and A. Gorgues, *Phys. Rev.* **B59** (1999) 9229.
- [15] B. Sahraoui, I.V. Kityk, M. Czerwinski and J. Kasperczyk, *High Performance Polymers*, **9** (1997) 51.
- [16] M. Czerwinski, J. Bieleninik, J. Napieralski, I.V. Kityk, J. Kasperczyk and R.I. Merwinski, *Europ. Polymer Journ.* **33** (1997) 1441.
- [17] M. Czerwinski, R.I. Merwinski, M. Kulesza, I.V. Kityk and J. Kasperczyk, *Materials Chemistry and Physics*, **205** (1998) 107.
- [18] R.I. Merwinski, I.V. Kityk, M. Makowska-Janusik, J. Straube, M. Matysiewicz and J. Kasperczyk, *Optical Materials* **6** (1996) 239.
- [19] J. Wasylak, E. Golis and I.R. Kityk, *J. Mater. Sci. Lett.* **16** (1997) 1870.
- [20] K.J. Plucinski, M. Makowska-Janusik, A. Mefleh, I.V. Kityk and V.G. Yushanin, *Mater. Sci. & Eng.* **B** (1999) (to be published).

H. KADDOURI*, M. MAKOWSKA-JANUSIK,
J. BERDOWSKI and I.V. KITYK

UV-INDUCED SHG in $\text{SiO}_x\text{C}_{1-x}\text{N}$ NANOCRYSTALS

Summary

A nonlinear optical effect of second harmonic generation has been revealed in SiOCN nanocrystallites incorporated into the oligoetheracrylates. With increasing power of photoinducing Q-switched nitrogen laser pulses ($\lambda=337$ nm), the SHG signal increases and achieves its maximum at pump photon flux of about 1.93 GW/cm^2 . The maximum photoinduced SHG is achieved for N/O ratio of about 0.92 and is equal to $(3.82 \pm 0.11) \text{ pm/V}$. Optimal concentration of the embedded SiOCN nanopowders lies between 1.2 % and 2.3 %. Decreasing temperature favors increase of the SHG. The key role of nanocrystallite interfaces is expected in observed nonlinear optical phenomena.